Iranian Journal of Oil & Gas Science and Technology, Vol. 4 (2015), No. 2, pp. 15-26
http://ijogst.put.ac.ir

Evaluation of the Effects of Nanoclay Addition on the Corrosion Resistance of Bituminous Coating

Hamid Reza Zamanizadeh[1], Mohammad Reza Shishesaz[1*], Iman Danaee[1], and Davood Zaarei[2]

[1] Department of Technical Inspection, Petroleum University of Technology, Abadan, Iran
[2] Technical Faculty, South Tehran Branch, Islamic Azad University, Tehran, Iran

Received: December 16, 2013*; revised*: January 01, 2014*; accepted*: January 04, 2014

Abstract

In this study, the corrosion resistance of a bituminous coating reinforced with different ratios of nanoclay pigment was studied. To make nanocomposite coatings, 2, 3, and 4 wt.% of clay (Cloisite Na^+) were incorporated into water emulsified bitumen. The coatings were applied to steel 37. Optical microscopy and X-ray diffraction (XRD) were used to characterize the nanocomposite structure. In order to investigate the anticorrosion behavior of the coatings, electrochemical impedance spectroscopy (EIS) and direct current polarization techniques were used. The results show that the coatings containing nanoclay have better performance compared to the neat bitumen. Moreover, it was revealed that the corrosion resistance of the nanocomposite increased as the clay loading increased up to 4 wt.%.

Keywords: Bitumen, Nanocomposite Coating, Clay, Corrosion

1. Introduction

Bitumen, obtained from petroleum refinery bottoms, is a thermoplastic containing bituminous materials. It has found widespread use in sealants, binders, waterproof coatings, and paving materials and it is preferred for its low cost, inherent cohesive nature, rheological properties, and thermal resistance (Çubuk et al., 2009).

Bitumen is a natural polymer of low molecular weight and like all polymers it is viscoelastic (Cheung, et al. 1997). Over the years, polymeric coatings have been developed due to their good barrier properties. However, pristine polymeric coatings are still permeable to corroding agents such as water, oxygen, and destructive ions like Cl^-, H^+, and SO_4^{2-}. In order to enhance the barrier properties of these polymeric coatings, many researchers have used various kinds of additives such as extenders and inorganic pigments (Nematollahi, et al. 2010). The addition of polymers to bitumen is known to impart enhanced service properties such as improved thermo-mechanical resistance, elasticity, and adhesive properties (Collins et al., 1991). However, polymer modified bitumens are expensive, difficult to operate, and incompatible (Polaccoa et al., 2005). Therefore, further efforts have been made for exploring new modifiers.

Recently, the layered silicates have been widely used for the modification of polymers (Ahmed et al., 2005). Layered silicate is a type of mineral with low cost and abundance. It consists of layers of

* Corresponding Author:
Email: shishesaz@put.ac.ir

tetrahedral silicate sheets and octahedral hydroxide sheets (Zilg et al., 2001). Polymer chains can intercalate into the interlayer of clay, which makes the clay dispersed into the polymer matrix on a nanometer scale. This leads to significant improvements in the thermal, mechanical, and barrier properties of polymers (Wanjale et al., 2003).

Montmorillonite (MMT)-modified bitumen composites have been successfully used to improve both the physical and rheological properties of modified bitumen (YU et al., 2007). However, previous research does not report any information on the effect of MMT on the anticorrosion properties of bitumen. This study investigates the corrosion protection behavior of natural montmorillonite clay/bitumen nanocomposite coatings.

2. Experimental results

2.1. Materials

Panels of steel 37 measuring 6.5 cm × 6.5 cm × 0.3 cm were used as the metallic substrates. The panels were sandblasted to Sa 2 ½ according to ASTM D609 and were kept in desiccator. Prior to coating, the panels were degreased with toluene and acetone. TW315 (TW315 is bitumen emulsified in water; the max volatile compound and max organic compound of TW315 are 60 wt.% and1 wt% respectively and its viscosity measured with Ford cup number 2 at 23° is between 30-60 seconds) complied with BS3416 type I as waterproof coating and the natural montmorillonite clay (Cloisite Na^+ or Na^+-MMT) as an additive were provided respectively by Tiva Company and Sothern Clay Product Company. Some properties of the latter are shown in Table 1.

Table 1
Natural montmorillonite nanoclay (Cloisite Na^+) pigment properties.

Particle size	Color	Density	Moisture content	X-ray Results (d001)
<25 µm	Off-white	2.86 g/cc	4-9%	1.17 nm

2.2. Preparation of nanocomposites

Three sets of nanocomposite samples containing 2, 3, and 4 wt.% of Cloisite Na^+ were prepared, as described below, through solvent intercalation technique.

At first the stoichiometric amounts of Cloisite Na^+ were added to 10 ml of distilled water to make 2, 3, and 4 wt.% mixtures. Then, by using a propeller, the mixtures were mechanically stirred at 1000 rpm for 120 min at room temperature followed by a sonication process for 90 min in an ice bath. The ultrasonic lab device UP200H (200W, 24 kHz) with an amplitude of 100 and a cycle gage of 1 was used for the sonication purpose. Secondly, the stoichiometric amounts of TW315 were added to the mixtures to make 2, 3, and 4 wt.% of nanocomposite coatings followed by 45 min mechanical blending. The coatings were labeled as PNC2, PNC3, and PNC4 where PNC stands for polymer nanocomposite and the number indicates the weight percent of clay used in the mixtures. The coatings were applied to the panels using 100 micrometer baker film applicator Elcometer model according to ASTM D823-95(2012). The thickness of dry film was 60±5 µm as measured by Elcometer 415.

2.3. Nanocomposite structural characterization

The optical homogeneity of the clay/water dispersion and the effects of sonication process on de-agglomeration of clay aggregates were examined using a BX-50 Olympus optical microscope.

It is also necessary to analyze the microstructure of the nanocomposites. XRD is one of the common techniques to characterize the microstructure of the prepared bitumen/clay nanocomposites to find out the intercalation or exfoliation of clays. The XRD experiments were performed in the range of 2θ=1° to 2θ=10° with X′Pert PRO MPD (PANalytical). The cobalt (Co) radiation (λ=1.78897 Å) was used as the XRD source.

2.4. Electrochemical measurements

Electrochemical impedance spectroscopy (EIS) is a nondestructive useful technique in studying, measuring, and estimating coating durability (Soer et al., 2009). The EIS measurements were performed using Auto lab PGSTAT 302N coupled with frequency response analyzer (FRA) 1260 over a frequency range of 100 kHz to 1 mHz with the 10-mV amplitude of sinusoidal voltage of open circuit potential. Fitting of experimental impedance spectroscopy data to the proposed equivalent circuit was done by a written least square code based on Marquardt method for the optimization of functions and Macdonald weighting for the real and imaginary parts of the impedance (Danaee, 2011; Macdonald, 1984). Three conventional electrode cells were used for the electrochemical measurements. A 3.5 wt.% NaCl solution was employed as the electrolyte. Coated panels acted as working electrode with an exposed area of 2.009 cm^2. A Pt electrode as the counter electrode and a saturated Ag/AgCl as the reference electrode were employed. The setup of the cell was placed in a Faraday cage.

The polarization measurements were obtained in 3.5 wt.% NaCl after 30 days of immersion. The data were recorded from below 200 mV to above 200 mV of the open circuit potential (E_{ocp}) at a scanning rate of 1 $mV.s^{-1}$. The polarization resistance (R_p) was calculated from Tafel plots according to Stern-Geary equation (Danaee et al., 2013; Ghasemi et al., 2013):

$$R_p = \frac{\beta_a.\beta_c}{2.303(\beta_a+\beta_c)} \times \frac{1}{I_{corr}} \quad (1)$$

where, β_a, β_c, and I_{corr} are anodic Tafel slope, cathodic Tafel slope, and corrosion current density respectively. The corrosion rate was also calculated through the following equation (Poorqasemi et al., 2009):

$$CR = \frac{0.0032 I_{corr} MW}{nd} \quad (2)$$

where, I_{corr}, MW, n, and d are corrosion current density ($\mu A.cm^{-2}$), molar mass ($g.mol^{-1}$), charge number, and density ($g.cm^{-3}$) of the tested metal respectively.

3. Results and discussion

3.1. Optical microscopy

Optical microscopy was used to ensure the dispersion of nanoclay in water before adding theme to the bitumen (TW315). First of all, the dispersion was made in the water containing 4 wt.% clay. Figure 1 presents the optical micrographs of 4 wt.% clay/water suspensions after 120 min of mechanical agitation and 60 min and 90 min of sonication process respectively in sections a, b, and c. Agglomerates were formed due to cohesive forces between clay stacks during the wetting process of clay with water. As shown in Figure 1(a), the mechanical agitation is a weak technique to overcome

these cohesive forces; thus a lot of clay is still agglomerated. Applying the sonication process and increasing the sonication time decreased the size and quantity of agglomerates (Figures 1(b) and 1(c)), which shows that sonication can cause the penetration of water molecules into the space between the sheets of clay. Therefore, the sonication process is an effective process to de-agglomerate clay stacks in the clay/water dispersion. Once clay dispersed in the 4 wt.% clay/water mixture, the abovementioned operations were also carried out for the other mixtures (the clay/water mixtures of 2 and 3 wt.%).

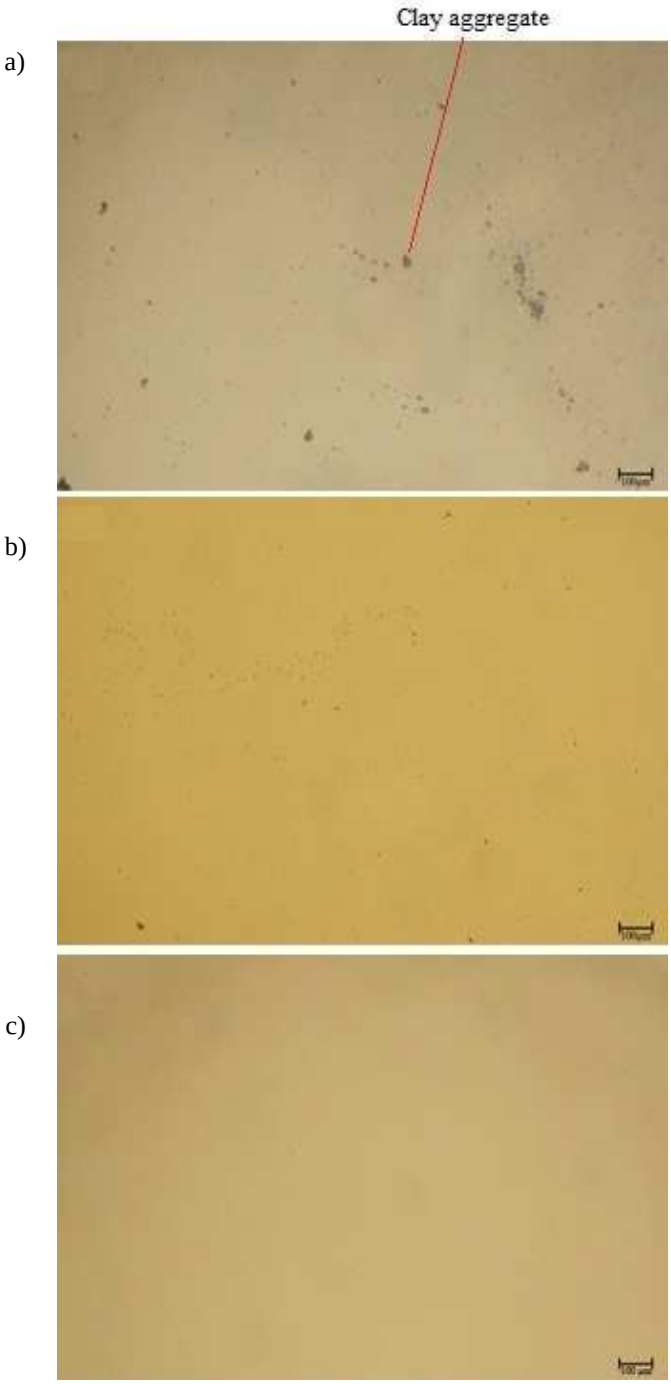

Figure 1
Optical micrographs of 4 wt.% clay/water suspensions: a) 120 min mechanical mixing; b) 60 min sonication; c) 90 min sonication.

3.2. X-ray diffraction (XRD)

The state of intercalation or exfoliation of nanoclay structure in bitumen matrix was studied using low angle X-ray diffraction (SAXS). Figure 2 shows the XRD patterns of 2, 3, and 4 wt.% clay-bitumen nanocomposites and pure Cloisite Na^+ used in this research. As displayed in Figure 2, pure Cloisite Na^+ has one peak at $2\theta=8.6095°$ according to Bragg's law. This peak is related to the d-spacing of 11.91694 Å of clay layers (this value is in agreement with the data sheet presented in Table 1 with a negligible difference). For the nanocomposite specimens containing 2 and 3 wt.% of nanoclay, there is no peak on their SAXS patterns, which confirms a great exfoliation of all the nanoclay in bitumen matrix for these two nanocomposites. However, in the case of the 4 wt.% clay-bitumen nanocomposite, one peak with a low intensity appeared on SAXS pattern at $2\theta=4.74195$, which is shifted to a lower angle compared with that of the pure Cloisite Na^+. This result shows that a considerable intercalation (according to Bragg's law d= 21.62158 Å) has occurred for some clays in the 4 wt.% clay-nanocomposite and the other clays exfoliated in the bitumen matrix. The high exfoliation of clays shows the nanoscale manner.

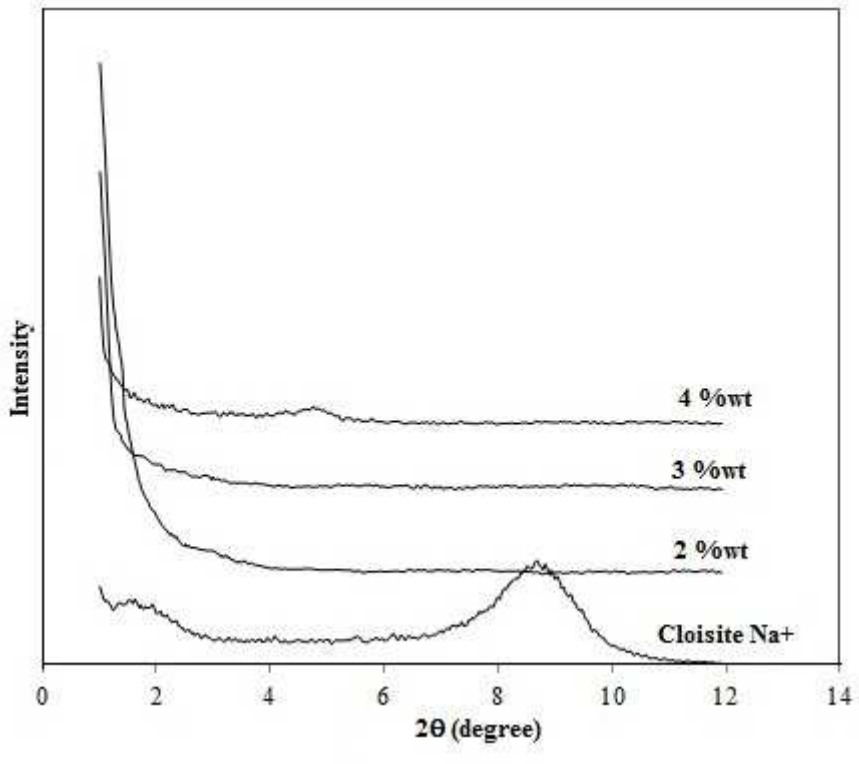

Figure 2
XRD patterns of pure Cloisite Na^+ and bitumen/clay nanocomposites

3.3. Electrochemical impedance spectroscopy (EIS)

Figures 3 to 6 show the Nyquist plots of coated steel at different immersion times and clay contents in a 3.5 wt.% NaCl solution. The plots show a depressed capacitive loop for all the coatings at low immersion times, which arises from the time constant of the resistance and capacitance of the coatings. The equivalent circuit compatible with the Nyquist diagram is depicted in Figure 7a. To obtain a satisfactory impedance simulation, it is necessary to replace the capacitor (C) with a constant phase element (CPE) Q in the equivalent circuit. Constant phase elements Q_c, R_s, and R_c correspond to

coating layer capacitance, solution resistance, and coating resistance respectively. The most widely accepted explanation for the presence of CPE behavior and depressed semicircles on solid electrodes is microscopic roughness, causing an inhomogeneous distribution in the solution resistance as well as in the double layer capacitance (Danaee and Niknejad Khomami et al., 2013; Danaee et al., 2011). To corroborate the equivalent circuit, the experimental data are fitted to the equivalent circuit and the circuit elements are obtained. Table 2 shows the equivalent circuit parameters for the impedance spectra at different clay loadings and immersion times. These results show that the addition of nanoadditives improves the coating resistance and the loop size decreases as the immersion time rises (Figures 3 and 4).

Table 2
Impedance data of nanocomposite coating at different contents and immersion times in a 3.5 wt.% NaCl solution.

Sample \ Immersion time		30 min.	14 Days	21 Days	60 Days
Neat bitumen	R_c (ohm)	1.8×10^{6}	4.2×10^{5}	3.3×10^{5}	1.7×10^{5}
	Q_c (F)	1.5×10^{-6}	5×10^{-6}	2×10^{-8}	1.5×10^{-8}
	n_1	0.75	0.6	0.65	0.65
	R_{ct} (ohm)			3.4×10^{6}	1.2×10^{6}
	Q_{dl} (F)			2×10^{-6}	1.3×10^{-5}
	n_2			0.63	0.65
PNC2 (2 wt.%)	R_c (ohm)	2.3×10^{6}	6.3×10^{5}	5.3×10^{5}	2.5×10^{5}
	Q_c (F)	3×10^{-6}	3×10^{-6}	4×10^{-6}	1.5×10^{-8}
	n_1	0.75	0.6	0.63	0.6
	R_{ct} (ohm)				1.3×10^{6}
	Q_{dl} (F)				1.5×10^{-6}
	n_2				0.6
PNC3 (3 wt.%)	R_c (ohm)	3.1×10^{6}	1.1×10^{6}	7.6×10^{6}	4.8×10^{5}
	Q_c (F)	2.1×10^{-6}	2×10^{-6}	3×10^{-6}	8×10^{-6}
	n	0.75	0.75	0.7	0.76
PNC4 (4 wt.%)	R_c (ohm)	5.1×10^{6}	1.4×10^{6}	1.1×10^{6}	6.9×10^{5}
	Q_c (F)	1.2×10^{-6}	1.9×10^{-6}	2×10^{-6}	4×10^{-6}
	n	0.75	0.83	0.72	0.74

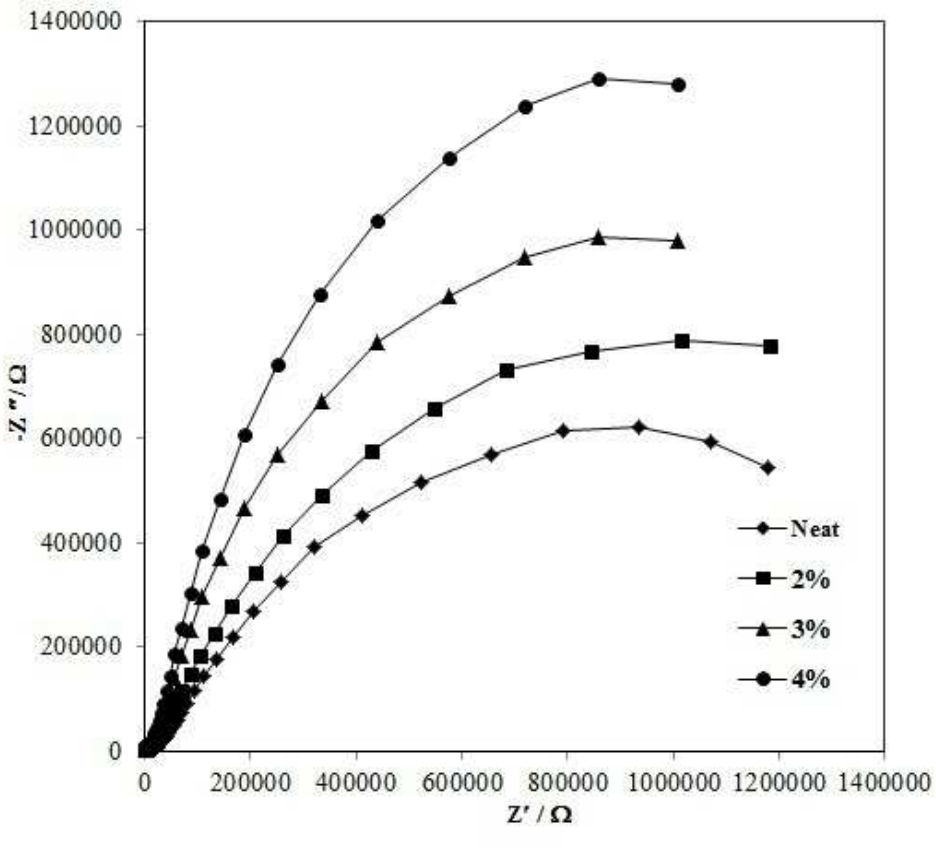

Figure 3
Nyquist diagrams of clay/bitumen coated samples after 30 min of immersion.

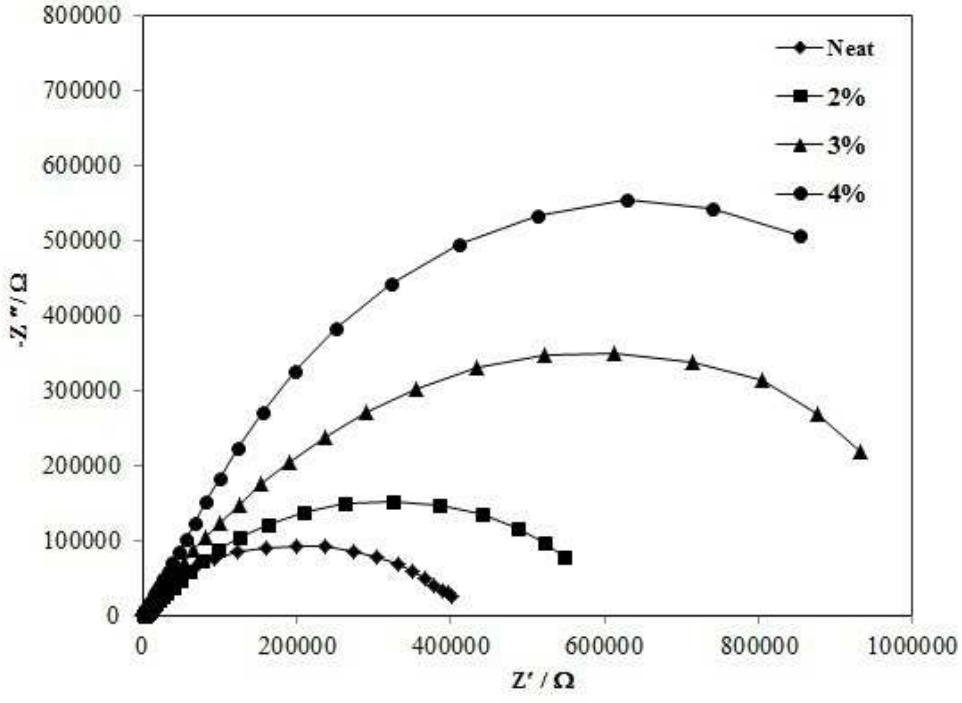

Figure 4
Nyquist diagrams of clay/bitumen coated samples after 14 days of immersion.

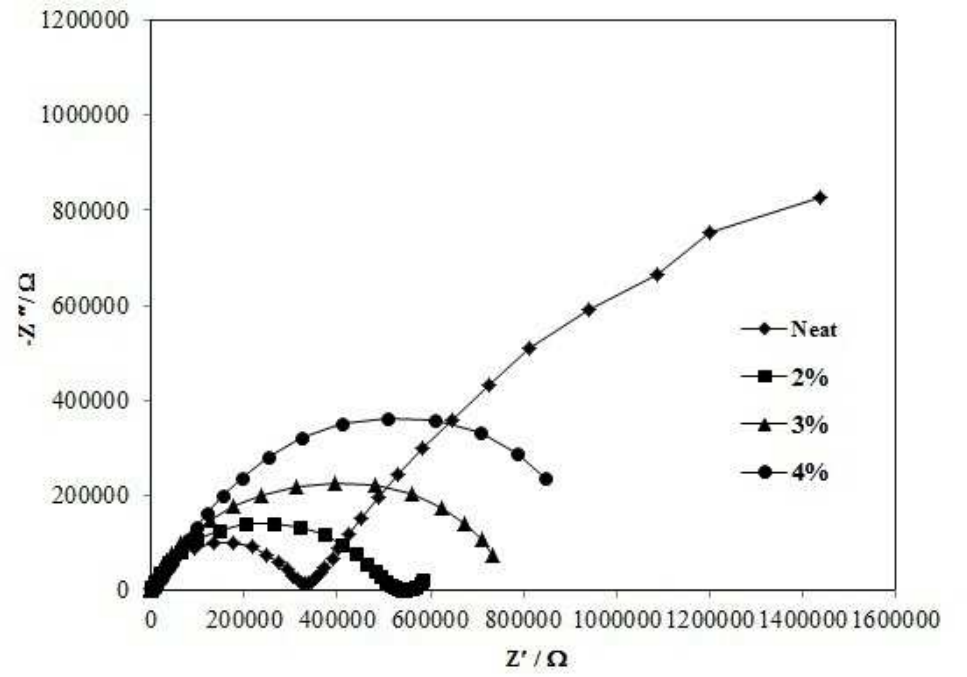

Figure 5
Nyquist diagrams of clay/bitumen coated samples after 21 days of immersion.

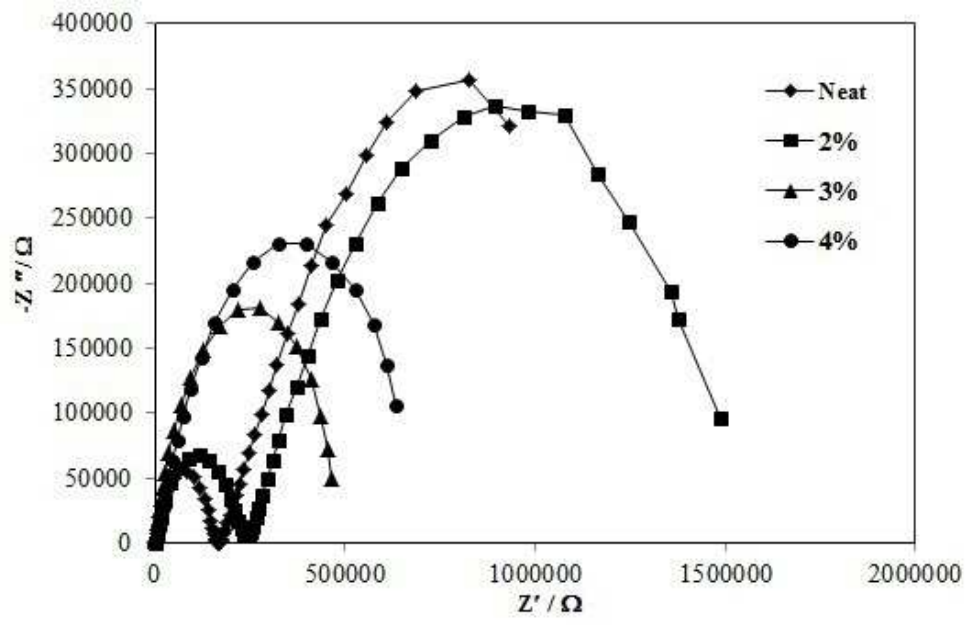

Figure 6
Nyquist diagrams of clay/bitumen coated samples after 60 days of immersion.

Twenty one days after immersion, neat bitumen and PNC2 started to create their second loop, which indicated that the corrosion began at the interface of the coatings and their substrates. Figure 7(b) shows the equivalent circuit compatible with these Nyquist diagrams, for which the corresponding parameters are tabulated in Table 2. Constant phase elements Q_{dl} and R_{ct} correspond to double layer capacitance $Q_{dl} = R^{n-1}C_{dl}^{n}$ (Danaee et al., 2010) and charge transfer resistance respectively.

Due to the higher stability of the coatings, only one capacitive loop was observed in samples PNC3 and PNC4 even after 60 days of immersion. For 60 days of immersion, sample PNC4 shows the highest R_c (R_c= 6.9×10^5) and thereby the best performance compared with the other coatings. By increasing the immersion time, Q_c increases (e.g. Q_c varies between 1.2×10^{-6} F to 4×10^{-6} F for PNC4), which is indicative of increased water penetrated into the coating, because water has a higher dielectric constant compared to the polymeric coatings (Deflorian et al., 1999).The conclusion is that adding nanoclay to bitumen forces corroding agents to travel a longer tortuous path to reach the substrate (Sun et al., 2008).

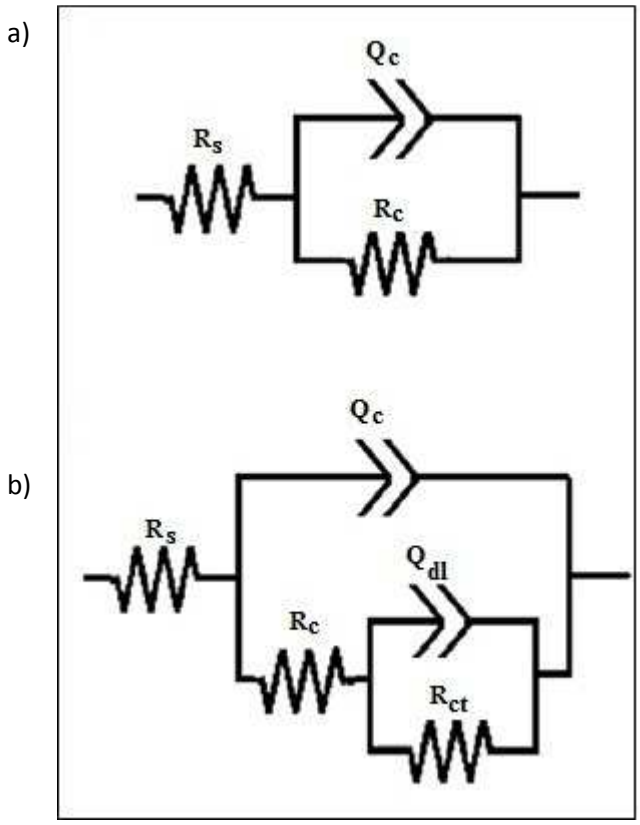

Figure 7
Equivalent circuits used for the numerical fitting of impedance plots obtained for the different immersion times; (a) before electrolyte reaches the metallic substrate and (b) after the initiation of corrosion process due to electrolyte penetration.

3.4. Potentiodynamic measurements

Figure 8 shows the Tafel polarization curves of the coated samples obtained after 30 days of immersion in a 3.5 wt.% NaCl solution. Tafel calculations are listed in Table 3, where E_{corr}, I_{corr}, CR, β_a, β_c, and R_p are the corrosion potential, corrosion current density, corrosion rate, anode Tafel constant, cathode Tafel constant, and polarization resistance respectively. The corrosion current density decreases while the corrosion potential rises as the amount of nanoclay increases. PNC4 has the most positive value of E_{corr} (-0.482 mv), the highest value of R_p (1.334 MΩ cm^{-2}), and the lowest value of I_{corr} (0.02485 μA.cm^{-2}), which confirms its enhanced corrosion protection properties. The enhancement of corrosion protection effect is related to the increase in the tortuosity of the diffusion pathways of corroding agents due to the presence of the dispersed silicate nanolayers (nanoclay).

Table 3
Potentiodynamic polarization parameters after 30 days of immersion of the samples.

Samples	$E_{corr.}$ (V)	R_p (MΩ.cm^{-2})	β_c (V.dec^{-1})	β_a (V.dec^{-1})	$I_{corr.}$ (μA.cm^{-2})	Corrosion rate (mm.year^{-1})
Neat bitumen	-0.588	0.1656	0.312	2.856	0.3675	0.004278
2 wt.% (PNC_2)	-0.556	0.3205	0.201	0.485	0.09426	0.001097
3 wt.% (PNC_3)	-0.544	0.8765	0.309	5.58	0.07217	0.0008402
4 wt.% (PNC_4)	-0.482	1.334	0.256	0.383	0.02485	0.0002893

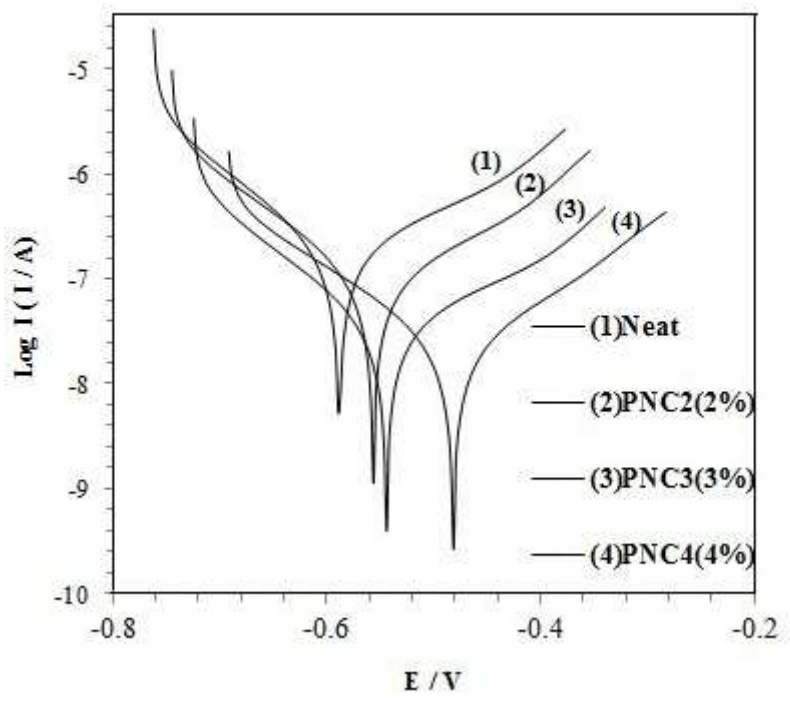

Figure 8
The polarization curves of the neat bitumen and the nanocomposite coatings after 30 days of immersion in a 3.5 wt.% NaCl solution.

4. Conclusions

Natural montmorillonite clay (Cloisite Na^+) was added to bitumen to make 2, 3, and 4 wt.% of clay/bitumen nanocomposite coatings. Optical microscopy showed that clay stacks were de-agglomerated in water and XRD results confirmed that the clay sheets were dispersed and separated in coatings layer, and that the clay particles were on nanoscale. EIS data revealed that the 4 wt.% clay/bitumen nanocomposite coating had the best performance with R_c= 6.9×10^5 after 60 days of immersion, and that the neat bitumen had the worst performance with R_c= 1.7×10^5 after 60 days of immersion..Potentiodynamic measurements revealed that the coating with 4 wt.% clay had the most positive value of corrosion potential (E= -0.482 V), and the lowest value of corrosion current density (I= 0.02485 μA.cm^{-2}) while the neat bitumen showed the least negative value of corrosion potential (E= -0.588 V) and the highest value of corrosion current density (I= 0.3675 μA.cm^{-2}) after 30 days of immersion in a 3.5 wt.% NaCl solution. Therefore, both EIS and polarization data proved that adding nanoclay improved the bituminous coatings resistance to corrosion ;in addition, they revealed that PNC4 had the best performance. The enhancement of corrosion protection was related to increasing the pathway of corroding agents to reach the substrate.

Nomenclature

EIS	: Electrochemical impedance spectroscopy
PNC	: Polymer nanocomposite
XRD	: X-ray diffraction
ASTM	: American society for testing and materials
C_{dl}	:Double layer capacitance
Q:	Constant phase element
R_{ct}	:Charge transfer resistance
C_c	: Coating capacitance
R_c	:Coating resistance

References

Ahmed, R. and Nehal, S., Nanocomposite Materials Based on Montmorillonite Clay Intercalated into Pristine Polyurethane, Material Science and Engineering A, Vol. 399, p. 368-376, 2005.

Cheung, C.Y., D. Cebon, and J. Mat, Deformation Mechanisms of Pure Bitumen, Civil Engineering, Vol. 9, p. 117-129, 1997.

Collins, J. H., Bouldin, M. G., Gelles, R., and Berker, A., Improved Performance of Paving grade Asphalts by Polymer Modification, Journal of the Association of Asphalt Paving Technologists, Vol. 60, p. 43-79, 1991.

Çubuk, M., Gürüa, M., and Kürsat Çubuk, M., Improvement of Bitumen Performance with Epoxy Resin, Fuel, Vol. 88, p. 1324-1328, 2009.

Danaee, I., Kinetics and Mechanism of Palladium Electrodeposition on Graphite Electrode by Impedance and Noise Measurements, Journal of Electroanalytical Chemistry, Vol. 662, p. 415-420, 2011.

Danaee, I., Ghasemi, O., Rashed, G. R., Rashvand Avei, M., and Maddahy, M. H., Effect of Hydroxyl Group Position on Adsorption Behavior and Corrosion Inhibition of Hydroxybenzaldehyde Schiff bases: Electrochemical and Quantum Calculations, Journal of Molecular Structure, Vol. 1035, p. 247-259, 2013.

Danaee, I., Niknejad Khomami, M., and Attar, A. A., Corrosion Behavior of AISI 4130 Steel Alloy in Ethylene glycol-water Mixture in the Presence of Molybdate, Materials Chemistry and Physics, Vol. 135, p. 658-667, 2010.

Danaee, I., Niknejad Khomami, M., and Attar, A. A., Corrosion of AISI 4130 Steel Alloy under Hydrodynamic Condition in Ethylene Glycol + Water + NO_2- Solution, Journal of Materials Science & Technology, Vol. 29, p. 89-96, 2013.

Danaee, I. and Noori, S., Kinetics of the Hydrogen Evolution Reaction on Ni-Mn Graphite Modified Electrode, International Journal of Hydrogen Energy, Vol. 36, p. 12102-12111, 2011.

Deflorian, F., Fedrizzi, L., and Rossi, S., Organic Coating Capacitance Measurement by EIS: Ideal and Actual Trends, Electrochimica Acta, Vol. 44, p. 4243-4249, 1999.

Ghasemi, O., Danaee, I. Rashed, G.R., Rashvand Avei, M. H., and Maddahy, M.H., The Inhibition Effect of Synthesized 4-Hydroxybenzaldehyde-1,3Propandiamine on the Corrosion of Mild Steel in 1 M HCl, Journal of Materials Engineering and Performance, Vol. 22, p. 1054-1063, 2013.

Macdonald, J.R., Note on the Parameterization of the Constant Phase Admittance Element, Solid State Ion, Vol. 13, p. 147-149, 1984.

Nematollahi, M., Heidarian, M., Peikari, M., Kassiriha, S. M., Arianpouya, N., and Esmaeilpour, M., Comparison between the Effect of Nanoglass Fake and Montmorillonite Organoclay on Corrosion Performance of Epoxy Coating, Corrosion Science, Vol. 52, p. 1809-1817, 2010.

Polaccoa, G., Berlincionia, S., Biondia, D., Stastnab, J., and Zanzotto, L., Asphalt Modification with Different Polyethylene-based Polymers, European Polymer Journal, Vol. 41, p. 2831-2844, 2005.

Poorqasemi, E., Abootalebi, O., Peikari, M., and Haqdar, F., Investigating Accuracy of the Tafel Extrapolation Method in HCl Solutions, Corrosion Science, Vol. 51, p. 1043-1054, 2009.

Soer, W. J., Ming, W., Koning, C. E., Van Benthem, R. A. T. M., Mol, J. M. C., and Terryn, H., Barrier and Adhesion Properties of Anti-corrosion Coatings based on Surfactant Free Latexes from Anhydride-containing Polymers, Progress in Organic Coatings, Vol. 65, p. 94-103, 2009.

Sun, L., Boo, W. J., and Clearfield, A., Barrier Properties of Model Epoxy Nanocomposites, Journal of Membrane Science , Vol. 318, p. 129-136, 2008.

Wanjale, S. D. and Jog, J.P. Effect of Modified Layered Silicates and Compatibilizer on Properties of PMP/clay Nanocomposites, Journal of Applied Polymer Science, Vol. 90, p. 3233-3238, 2003.

YU, J. Y., Zeng, X., and WU, S. P., Preparation and Properties of Montmorillonite Modified Asphalts, Materials Science and Engineering A, Vol. 47, p. 233-238, 2007.

Zilg, C., Dietsche, F., Hoffmann, B., Dietrich, C., and Mulhaupt, R., Nanofillers based upon Organophilic Layered Silicates, Macromolecular Symposia, Vol. 169, p. 65-77, 2001.